Environmental Pollution xxx (2016) 1–11

Contents lists available at ScienceDirect

Environmental Pollution

journal homepage: www.elsevier.com/locate/envpol

Characterization and source apportionment of size-segregated atmospheric particulate matter collected at ground level and from the urban canopy in Tianjin☆

Jiao Wang [a], Ming Zhou [a], Bao-shuang Liu [a], Jian-hui Wu [a, *], Xing Peng [a], Yu-fen Zhang [a], Su-qin Han [b], Yin-chang Feng [a], Tan Zhu [a]

[a] State Environmental Protection Key Laboratory of Urban Ambient Air Particulate Matter Pollution Prevention and Control, College of Environmental Science and Engineering, Nankai University, Tianjin 300071, China
[b] Tianjin Institute of Meteorological Science, Tianjin 300074, China

ARTICLE INFO

Article history:
Received 13 July 2016
Received in revised form
24 October 2016
Accepted 25 October 2016
Available online xxx

Keywords:
Size distribution
Particulate matter
Chemical composition
Urban canopy
Source apportion

ABSTRACT

To investigate the size distributions of chemical compositions and sources of particulate matter (PM) at ground level and from the urban canopy, a study was conducted on a 255 m meteorological tower in Tianjin from December 2013 to January 2014. Thirteen sets of 8 size-segregated particles were collected with cascade impactor at 10 m and 220 m. Twelve components of particles, including water-soluble inorganic ions and carbonaceous species, were analyzed and used to apportion the sources of PM with positive matrix factorization. Our results indicated that the concentrations, size distributions of chemical compositions and sources of PM at the urban canopy were affected by regional transport due to a stable layer approximately 200 m and higher wind speed at 220 m. The concentrations of PM, Cl^- and elemental carbon (EC) in fine particles at 10 m were higher than that at 220 m, while the reverse was true for NO_3^- and SO_4^{2-}. The concentrations of Na^+, Ca^{2+}, Mg^{2+}, Cl^- and EC in coarse particles at 10 m were higher than that at 220 m. The size distributions of major primary species, such as Cl^-, Na^+, Ca^{2+}, Mg^{2+} and EC, were similar at two different heights, indicating that there were common and dominant sources. The peaks of SO_4^{2-}, NH_4^+, NO_3^- and organic carbon (OC), which were partly secondary generated species, shifted slightly to the smaller particles at 220 m, indicating that there was a different formation mechanism. Industrial pollution and coal combustion, re-suspended dust and marine salt, traffic emissions and transport, and secondary inorganic aerosols were the major sources of PM at both heights. With the increase in vertical height, the influence of traffic emissions, re-suspended dust and biomass burning on PM weakened, but the characteristics of regional transport from Hebei Province and Beijing gradually become obvious.

1. Introduction

Atmospheric particulate matter (PM) is the primary air pollutant in most urban areas of China, which plays an important role in the deterioration of air quality, in the impairment of visibility and human health, and in changing the radiative balance directly and indirectly (Pope and Dockery, 2006; Watson, 2002; Wang and Xie, 2009; Bellouin et al., 2005; Ramachandran and Kedia, 2010). All of these effects depend strongly on the size distributions and chemical compositions of atmospheric particles (Contini et al., 2014; Zhao et al., 2011; Yang et al., 2015). However, previous studies that focused on the size distributions and associated chemical species of PM were conducted at ground level (5–10 m), which is influenced mostly by human activities on a street scale (Yao et al., 2003; Zhao et al., 2011; Chan et al., 2000). An observation of size-segregated atmospheric particulate matter on urban scales (200–300 m) is necessary for understanding the sources, transport, transformation, and removal mechanisms of particles (Wang et al., 2014c; Han et al., 2015; Wu et al., 2015; Deng et al., 2015; Sun et al.,

☆ This paper has been recommended for acceptance by Yele Sun.

* Corresponding author. State Environmental Protection Key Laboratory of Urban Ambient Air Particulate Matter Pollution Prevention and Control, College of Environmental Science and Engineering, Nankai University, No. 94 Weijin Road, Tianjin 300071, China.
E-mail address: envwujh@nankai.edu.cn (J.-h. Wu).

http://dx.doi.org/10.1016/j.envpol.2016.10.069
0269-7491/

2015). Reasonable control measures can be taken based on the characteristics of the particle size distribution and the results of source apportionment at ground level and in the urban canopy (Zhao et al., 2011).

Tianjin is located in the Beijing-Tianjin-Hebei region, where the air pollution condition is the most serious in China (Sun et al., 2014, 2016). Secondary aerosols, coal combustion, traffic, industrial sources and crustal dust are the main sources of PM in the area (Zíkova et al., 2015; Yang et al., 2016; Huang et al., 2014; Wu et al., 2015; Wang et al., 2014b). There are relatively systematic observations of atmospheric particulate matter and meteorological parameters on a 255 m meteorological tower located in the Tianjin Meteorological Bureau (Han et al., 2015; Gao et al., 2012; Huang et al., 2009). A series of studies about the vertical characteristics of atmospheric particulate matter have been conducted in Tianjin, such as the vertical characteristics of carbonaceous species and their source contributions (Shi et al., 2012), the vertical characteristics of levels and potential sources of water-soluble ions in PM_{10} (Tian et al., 2013), the vertical characteristics of $PM_{2.5}$ during the heating season (Wu et al., 2015) and so on. There are different formation, transformation, transport, and removal mechanisms in different mode particles (Zhao et al., 2011; Whitby, 1978; Hering and Friedlander, 1982). The size distributions of chemical compositions can provide detailed information on the formation and origin of particles (Yao et al., 2003; John et al., 1990; Hering et al., 1997; Ondov and Wexler, 1998). However, studies that have focused on investigating the size distribution of chemical compositions and sources of particulate matter (PM) in different mode at ground level and from the urban canopy have not yet been conducted.

In this study, a novel campaign was carried out on a 255 m meteorological tower in Tianjin from December 2013 to January 2014. Thirteen sets of size-segregated atmospheric particles were collected at 10 m and 220 m. Twelve components of particulates, including water-soluble inorganic ions (Na^+, NH_4^+, K^+, Mg^{2+}, Ca^{2+}, F^-, Cl^-, NO_2^-, NO_3^- and SO_4^{2-}) and carbonaceous species (elemental carbon (EC) and organic carbon (OC)), were analyzed. Positive matrix factorization (PMF) was used to apportion the sources of PM in different mode. The objectives of this paper are as follows: (1) to investigate and compare the size distribution of the chemical species of particulate matter at ground level and from the urban canopy and (2) to apportion and compare the source contributions to size-segregated particles measured at two different heights.

2. Experimental techniques and methods

2.1. Sample collection

Tianjin (39°10′ N, 117°10′ E) is an international coastal megacity with over 14 million people in 11,706 km^2. Tianjin experiences a sub-humid warm temperate monsoon climate, with an annual average temperature of 14 °C and annual average rainfall of 600 mm. Lower temperatures, lesser precipitation and stronger northwest winds often occur in winter. In this study, aerosol samples and meteorological data were collected at heights of 10 m and 220 m heights on a 255 m meteorological tower synchronously. The tower is located in a district with a mixture of residential, commercial and traffic areas. The specific location of sampling site is shown in Fig. 1.

Sampling was performed from December 2013 to January 2014 using an 28.3 L min^{-1} eight-stage Anderson Cascade impactor (Thermo Electron, America, model E-0162) in the following size ranges: (1) 0.4–0.7 μm, (2) 0.7–1.1 μm, (3) 1.1–2.1 μm, (4) 2.1–3.3 μm, (5) 3.3–4.7 μm, (6) 4.7–5.8 μm, (7) 5.8–9.0 μm, and (8) 9.0–10 μm (aerodynamic diameter) (Xue et al., 2011; Heeinrich et al., 2003; Ian Colbeck, 2010, 2012; Sannigrahi et al., 2006). Two parallel samplers were set at the heights of 10 m and 220 m in order to collect particulate matter on quartz-fiber filters for a subsequent soluble ionic/carbon component analysis. In order to obtain sufficient particulate matter at each stage to weigh and analyze, samplers were continuous operating for 47 h from 09:00 a.m. to 08:00 a.m. of the third day (China Standard Time, UTC + 08:00). A total of 13 sets of samples were obtained.

2.2. Gravimetric and chemical analysis

Before sampling, the quartz fiber filters were baked in an oven at 400–500 °C in order to remove organic compounds in the unloaded fiber. Before weighing, loaded and unloaded filters were equilibrated for 48 h under constant temperature (20 ± 1 °C) and RH (40 ± 3%). Using a sensitive microbalance (METTLER TOLEDO, Switzerland, model AX205) with a resolution of 10 μg, all filters were weighed more than twice until the difference of two repeated measures was less than±15 μg. After weighing, filters were stored at −4 °C for the subsequent component analysis.

The water-soluble inorganic ions were analyzed for Na^+, NH_4^+, K^+, Mg^{2+}, Ca^{2+}, F^-, Cl^-, NO_2^-, NO_3^- and SO_4^{2-} using ion chromatography (Thermo, America, model ICS-900). First, a quarter of the filter was extracted into 5 mL of deionized water in an ultrasonic bath (GT sonic, China, GT-2120QTS) at a frequency of 40 kHz for 15 min. Then, 1 mL of supernatant solution was drawn into a syringe and filtrated by a disposable filter head with pore size of 0.22 μm before being injected into the ion chromatograph. Last, water-soluble inorganic ions were identified with the solution flowing through the cation and anion column. Before the analysis of water-soluble inorganic ions, the standard solutions were detected for three times and low relative standard deviations could be observed. The EC and OC were analyzed with the thermal optical carbon analyzer (Desert Research Institute, America, model 2001) with the IMPROVE A thermal/optical reflectance protocol. A 0.53 cm^2 wafer was cut off from the rest quartz filter and was sent into the thermal optical carbon analyzer. The first sample was reanalyzed every ten samples and the precision was below 2%. The calibration of the analyzer was done before and after sample analysis for every day.

Hourly data for temperature (T), wind speed (WS) and relative humidity (RH) were synchronously measured at 14 platforms (5, 10, 20, 30, 40, 60, 80, 100, 120, 140, 160, 180, 200 and 220 m) by an automatic weather station installed on the tower.

2.3. PMF model

In this study, EPA PMF 5.0 software was used to apportion the sources of size-segregated atmospheric particles. PMF is one of the well-established and widely used receptor models for the source apportionment of atmospheric particulate matter (Paatero and Tapper, 1994; Viana et al., 2008; Tian et al., 2013). It has distinct advantage in its ability to accommodate the dataset which is missing or below detection limit. The PMF model has been successfully applied and its detailed description can be found in previous studies (Paatero and Tapper, 1993, 1994; Chueinta et al., 2000; Song et al., 2001). In addition, it has been proven to be successfully applied to datasets with size-segregated atmospheric particles (Gietl and Klemm, 2009; Contini et al., 2014; Tan et al., 2014; Amato et al., 2009). In this study, the concentrations of water-soluble inorganic ions and carbonaceous species of all size fractions (208 sets) were input to the PMF 5.0 software. S/N is the signal-to-noise ratio and is used to address weak and bad variables when performing PMF (Paatero and Hopke, 2003). The signal vector is denoted as S and the noise vector is denoted as N. Next, S/N is

Please cite this article in press as: Wang, J., et al., Characterization and source apportionment of size-segregated atmospheric particulate matter collected at ground level and from the urban canopy in Tianjin, Environmental Pollution (2016), http://dx.doi.org/10.1016/j.envpol.2016.10.069

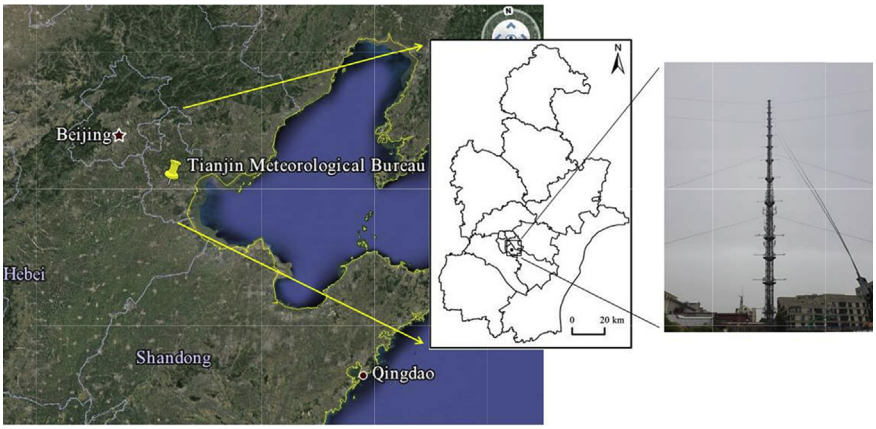

Fig. 1. Location of the sampling site in Tianjin.

defined as Eq. (1). Variables with very low S/N (≤0.2) were excluded from the analysis, while weak variables (0.2 ≤ S/N ≤ 2.0) were down-weighted (Ancelet et al., 2012). In this paper, the S/N of Mg^{2+}, Ca^{2+}, F^-, NO_2^- and NO_3^- was lower than 2.0, and these species were set as weak variables.

$$S/N = \sqrt{\sum s_i^2 / \sum n_i^2} \quad (1)$$

where i in the formula is the chemical composition of PM.

2.4. Trajectory cluster analysis

In order to evaluate the origin and transport of air masses, 36-h air mass back-trajectories were calculated at 200 m above the ground with the Hybrid Lagrangian Single-Particle Integrated Trajectory (HYSPLIT4) model (Long et al., 2014; Yang et al., 2015). The meteorological data (downloaded from the website of the US National Centers for Environmental Prediction, and accessible at ftp://arlftp.arlhq.noaa.gov/pub/archives/reanalysis) was used in HYSPLIT4 calculations during the sampling period. Back-trajectories were simulated at 00:00, 06:00, 12:00 and 18:00 (Universal Time Coordinated (UTC)) for each sampling day. All trajectories were clustered with the HYSPLIT clustering algorithm.

3. Results and discussion

3.1. Mass size distributions of PM

The fitting lines of the average mass size distributions of PM at the heights of 10 m and 220 m are shown in Fig. 2. A similar bimodal distribution pattern could be found at two different heights, in which the peak value appeared in the size bins of 0.7–1.1 μm and 9.0–10.0 μm, respectively. In this study, particles in the size bin of 0.4–2.1 μm were defined as fine particles, and the mass concentration of fine particles was calculated by summing up the concentrations of $PM_{0.4\text{-}0.7}$, $PM_{0.7\text{-}1.1}$ and $PM_{1.1\text{-}2.1}$. Particles in the size bin of 2.1–10.0 μm were defined as coarse particles, and the mass concentration of coarse particles was calculated by summing up the concentrations of $PM_{2.1\text{-}3.3}$, $PM_{3.3\text{-}4.7}$, $PM_{4.7\text{-}5.8}$, $PM_{5.8\text{-}9.0}$ and $PM_{9.0\text{-}10.0}$. The averaged mass concentrations of fine particles and coarse particles at 10 m were 105.9 ± 65.7 μg m^{-3} and 118.8 ± 28.9 μg m^{-3}, which were 8.1% and 10.4% higher than the 98.0 ± 69.1 μg m^{-3} and 107.6 ± 35.9 μg m^{-3} measured at 220 m, respectively. The concentrations of fine particles were about three times of the annual standard (35 μg m^{-3}) for GroupII area (National Ambient Air Quality Standards, GB 3095-2012). On average, fine

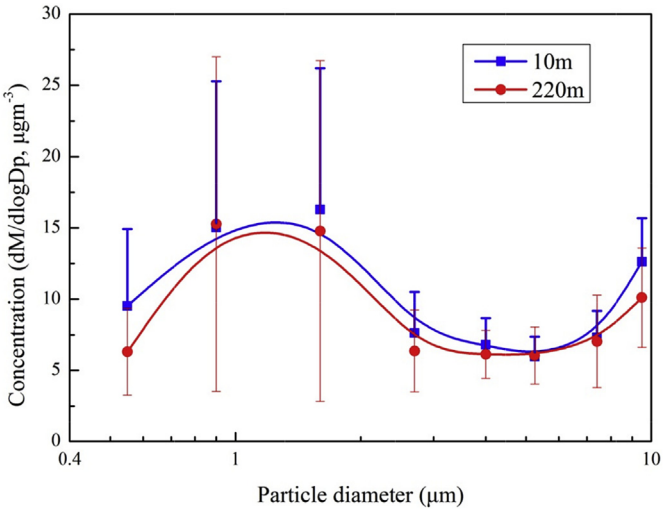

Fig. 2. Average mass size distributions of particulate matter at the heights of 10 m and 220 m.

particles accounted for the similar proportion (47%) of the PM_{10} mass at both heights. Overall, a general deceasing trend of PM concentrations was shown with increasing height. It is similar with researches conducted in Beijing (Sun et al., 2015) and Guangzhou (Deng et al., 2015).

The vertical profiles of meteorological variables during the sampling period are shown in Fig. 3. The temperature at 220 m was 1.1 °C lower than that at 10 m, and a clear inversion of T could be observed at approximately 200 m. The wind speed WS was relatively constant between 200 and 220 m (5.1 ± 1.6 m s^{-1}), which was five times higher than that at 10 m (1.0 ± 0.2 m s^{-1}). The RH showed a large increase to 62% at 60 m, while it was 9.1% higher at 220 m that at 10 m (56.6 ± 15.1%). There was a stable layer approximately 200 m due to the strong temperature inversion and higher RH, which could lead to a delay in the diffusion of air pollutants between the ground level and 220 m. Higher WS at 220 m strengthened the horizontal transport of atmospheric particulate matter in the urban canopy. The higher WS at 220 m also indicated the top of tower was under the influence of regional transport.

3.2. Size distribution of chemical composition

There were obviously compositional differences between fine particles and coarse particles. As shown in Fig. 4, OC, SO_4^{2-}, NO_3^-,

Please cite this article in press as: Wang, J., et al., Characterization and source apportionment of size-segregated atmospheric particulate matter collected at ground level and from the urban canopy in Tianjin, Environmental Pollution (2016), http://dx.doi.org/10.1016/j.envpol.2016.10.069

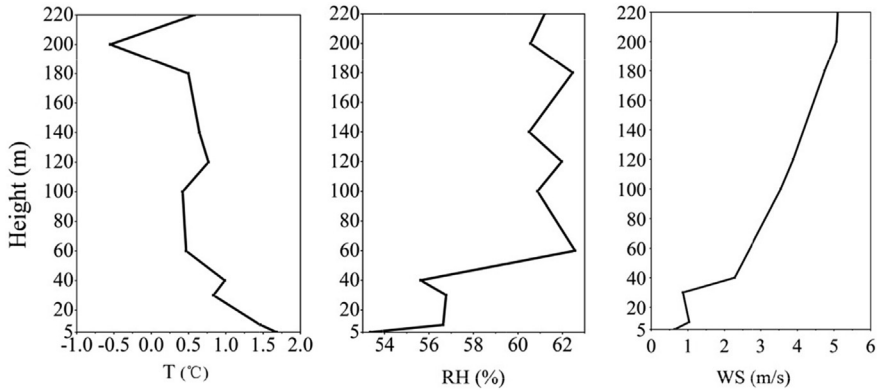

Fig. 3. Average vertical profiles of T, RH, and WS.

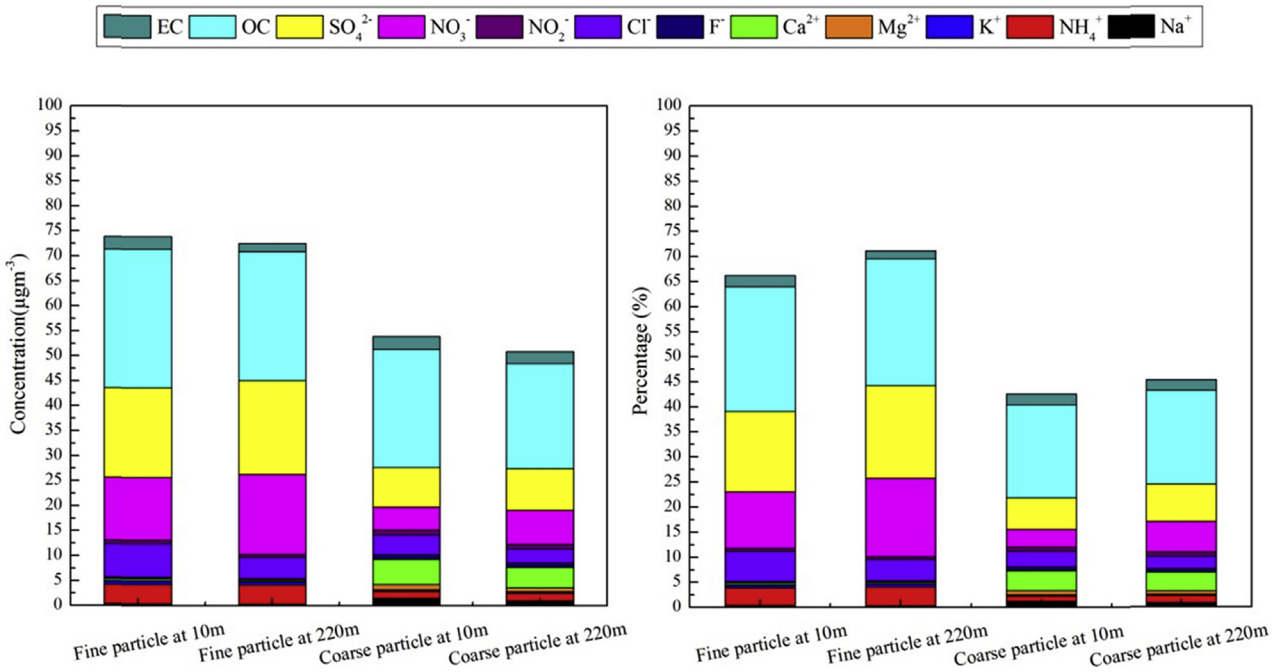

Fig. 4. Concentrations and percentages of the twelve components in fine-mode and coarse-mode particles at different heights.

Cl^-, NH_4^+ and EC were the principal chemical compositions of fine particles, accounting for 24.9%, 16.0%, 11.3%, 6.0%, 3.5% and 2.2% of $PM_{2.1}$ at 10 m. Coarse particles were mostly consisted of OC, SO_4^{2-}, NO_3^-, Cl^-, Ca^{2+} and EC, with the percentages of 28.6%, 6.3%, 3.6%, 3.2%, 3.9% and 2.1% to $PM_{2.1}$ at 10 m. The percentages of K^+, Mg^{2+}, F^- and NO_2^- to PM were all below 1% in both modes. The concentrations of SO_4^{2-}, NO_3^- and NH_4^+ in fine particles were higher than that in coarse particles, while the concentrations of Ca^{2+} in coarse particles were higher than that in fine particles. It suggested that secondary inorganic aerosols were mainly concentrated in fine particles. The fraction of ions and carbonaceous species in PM at 220 m was 7% higher than that at 10 m, though the total concentration of ions and carbonaceous species at 220 m was 3.6% lower than that at 10 m. This result indicated that the proportion of ions and carbonaceous species in PM rose with the increase in height, especially for SO_4^{2-} and NO_3^-.

The cation and anion equivalents were calculated based on Eq. (2) and Eq. (3) (Long et al., 2014). The ratio of C/A ($R_{C/A}$) was widely applied to evaluate the neutralizing level of PM. The average values of $R_{C/A}$ at 10 m were 0.52 and 1.37 for fine and coarse particles, while those at 220 m were 0.50 and 1.40, respectively. These results indicated that neutralizing level of PM was quite similar at 10 m and 220 m. The formation of abundant acidic secondary aerosols in fine particles may be one reason for the low value of $R_{C/A}$ (Long et al., 2014). In addition, the NH_4^+ loss on the filters may be another reason for the imbalance in ions of fine particles (Appel et al., 1984; Dasch et al., 1989; Harrison et al., 1990; Pathak and Chan, 2005). The species (such as CO_3^{2-} and HCO_3^-) that were not analyzed contributed to a deficit of anions in coarse particles (Shen et al., 2008). The size distribution of chemical composition could reflect its origins and atmospheric processes directly. Further investigation about the size distribution of major chemical compositions has been shown as follows.

$$C_{(cation\ equivalents)} = Na^+/23 + K^+/39 + Mg^{2+}/12 + Ca^{2+}/20 + NH_4^+/18 \quad (2)$$

Please cite this article in press as: Wang, J., et al., Characterization and source apportionment of size-segregated atmospheric particulate matter collected at ground level and from the urban canopy in Tianjin, Environmental Pollution (2016), http://dx.doi.org/10.1016/j.envpol.2016.10.069

$$A_{\ (\ anion\ equivalents\ )} = Cl^{-}\Big/35.5 + F^{-}\Big/19 + NO_2^{-}\Big/46 + NO_3^{-}\Big/62 + SO_4^{2-}\Big/48 \quad (3)$$

where the numerical value mentioned in the formula was the molar mass of the ion, in the units of g mol^{-1}.

3.2.1. Na^+, K^+ and Cl^- size distributions

As shown in Fig. 5, the size distributions of Na^+ and Cl^- at the two different heights were similar. Na^+ was found to have a single mode that peaked at 9–10 μm. Cl^- was found to have a bimodal mode. The stronger peak for Cl^- appears in the size bin of 0.7–1.1 μm and the weaker peak was located at 9–10 μm. More than 75% of Na^+ was concentrated in coarse particles, while 60% of Cl^- was concentrated in fine particles. Sea-salt was the major source of Na^+ and Cl^- in coarse particles (Herner et al., 2006; Quinn et al., 2004; Kumar et al., 2008). Therefore, there must be another significant formation mechanism of Cl^- in addition to sea salt. Cl^- in fine particles might come from waste incineration (Kaneyasu et al., 1999), coal burning (Zhao et al., 2011), biomass burning (Cao et al., 2015), secondary aerosol formation (Zhao and Gao, 2008) and long-range transport (Zhao et al., 2010).

The distribution of potassium was a unimodal pattern that peaked at 0.7–1.1 μm. Potassium is usually regarded as a tracer for biomass burning. Non-sea-salt potassium (nss-K^+) were calculated based on Eq. (4) (Cao et al., 2015). The values of nss-K+/$PM_{2.1}$ at 10 m and 220 m were closed (0.016) and lower than that derived from biomass burning (0.024) (Cao et al., 2015). The correlation of nss-K^+ to $PM_{2.1}$ (R^2 = 0.21) was weak, while a better correlation

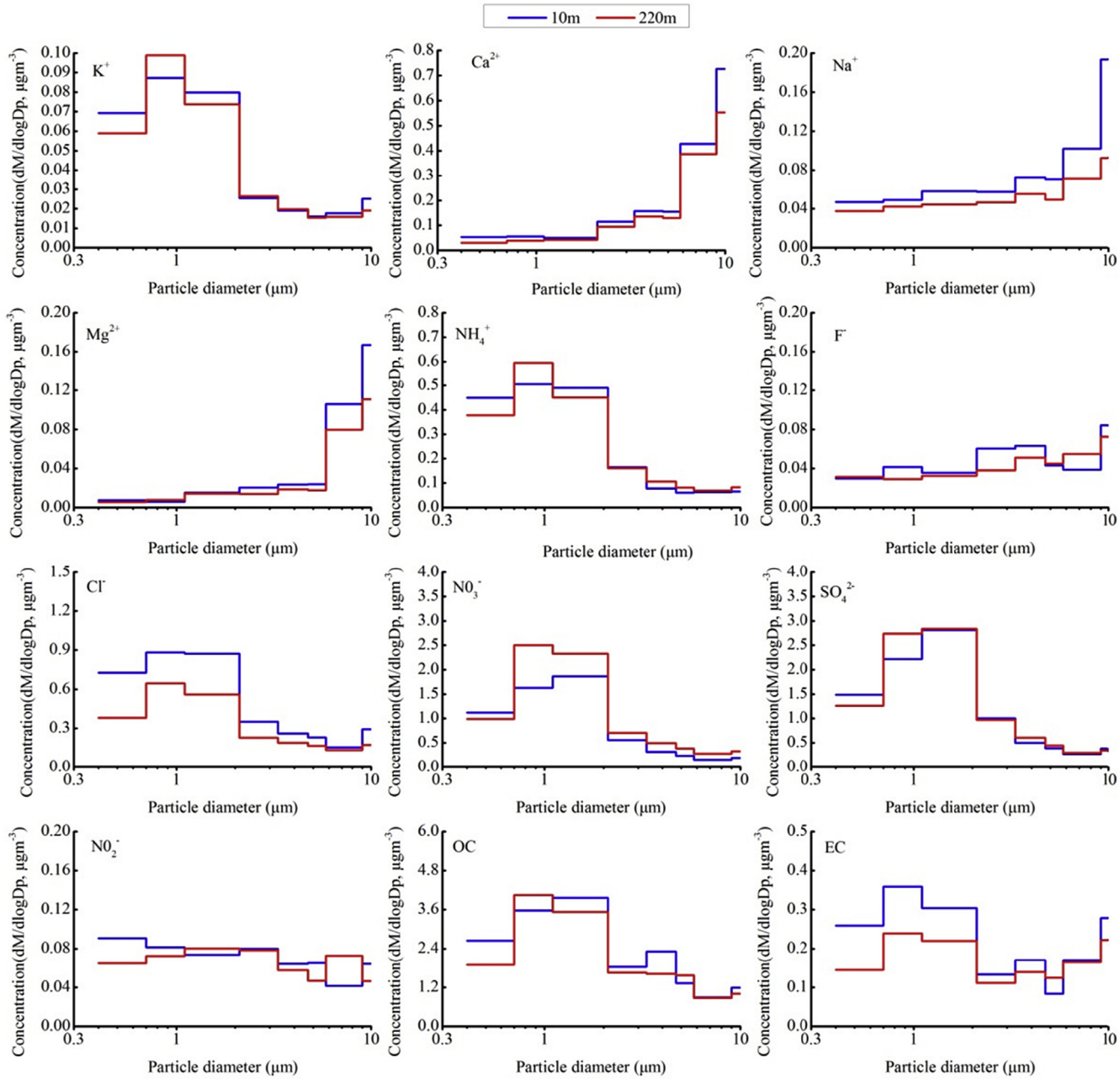

Fig. 5. Average size distributions of chemical species measured at 10 m and 220 m.

Please cite this article in press as: Wang, J., et al., Characterization and source apportionment of size-segregated atmospheric particulate matter collected at ground level and from the urban canopy in Tianjin, Environmental Pollution (2016), http://dx.doi.org/10.1016/j.envpol.2016.10.069

could been seen between nss-K^+ and Cl^- (R^2 = 0.46). The concentration of Cl^- at 10 m was 51% higher than that at 220 m, especially in fine particles. It indicated that local source emissions, such as crude coal and biomass burning contributed the most to chloride in fine particles.

$$C_{nss-K^+} = C_{K^+} - 0.0355 C_{Na^+} \quad (4)$$

3.2.2. Ca^{2+} and Mg^{2+} size distributions

As shown in Fig. 5, Ca^{2+} and Mg^{2+} were found to have a single mode that peaked at 9–10 μm at both heights. More than 90% of Ca^{2+} and Mg^{2+} were concentrated in coarse particles. Ca^{2+} and Mg^{2+} in coarse mode mainly come from soil particles or falling dust (Arimoto et al., 1996). In addition, construction dust is another source for Ca^{2+} (Wang et al., 2005). Mineral dust and sea salts also contribute to the coarse-mode Mg^{2+}. As shown in Table S1 which is provided in the supplementary materials, good correlations between Ca^{2+} and Mg^{2+} were found at both heights (R^2 = 0.95 at 10 m and 0.94 at 220 m), revealing that the sources of Ca^{2+} and Mg^{2+} were similar. There were relatively good correlations between Na^+ and Mg^{2+} (R^2 = 0.83 at 10 m and 0.77 at 220 m), revealing that sea salt also contributed to Mg^{2+}. The concentrations of Ca^{2+} and Mg^{2+} at 10 m were 22.5% and 37.8% higher than that at 220 m, respectively.

3.2.3. SO_4^{2-}, NO_3^- and NH_4^+ size distributions

As shown in Fig. 5, the size distributions of sulfate at both heights were similar, which was a strongly unimodal pattern that peaked at 1.1–2.1 μm. Sulfate was mainly concentrated in fine particles at both heights, accounting for the same proportion (69%) of the sulfate mass in PM_{10}. Sulfate in fine particles mainly originates from secondary sources, coal burning, traffic emissions, biomass burning, or long-range transport (Zhuang et al., 1999; Yamasoe et al., 2000; Herner et al., 2006; Anlauf et al., 2006). Fine particles are considered to be emitted from biomass burning when the concentration ratio of potassium to sulfate is larger than one (Kleeman et al., 1999; Yamasoe et al., 2000). The average ratios of potassium to sulfate at 10 m and 220 m were 0.04 and 0.03 in fine particles, respectively. In addition, a weak correlation could be found between the mass concentrations of sulfate and potassium in fine particles. All this information indicated that biomass burning was not a dominant source of sulfate in fine particles in Tianjin. A mass ratio of sodium to sulfate of 0.05 in fine particles is used to estimate the contribution of traffic to sulfate (Anlauf et al., 2006). In this study, the mean ratios at 10 m and 220 m were 0.023 and 0.018, respectively. This indicated that secondary sources, coal burning and long-range transport contributed the most to sulfate in fine particles.

In keeping with the distribution of sulfate, nitrate and ammonium also had a strongly unimodal pattern that peaked at 0.7–1.1 μm, while the peak of nitrate shifted to 1.1–2.1 μm at 10 m. Additionally, nitrate and ammonium were mainly concentrated in fine particles in this study. The proportion of fine-mode nitrate and ammonium (74% and 74%) to the nitrate and ammonium mass in PM_{10} at 10 m was higher than that at 220 m (70% and 71%).

In addition to that emitted directly from traffic vehicles and long-range transport, there are two pathways to explain the formation of fine mode nitrate: (1) Nitrate in fine particles is formed through homogeneous gas-phase reactions in which NOx is oxidized to nitric acid (HNO_3). Then, ammonium nitrate is formed through a process in which HNO_3 reacts with ammonia (NH_3). (2) Nitrate in fine particles is formed through heterogeneous reactions in which HNO_3 reacts with pre-existing fine particles (Zhuang et al., 1999; Zhao et al., 2011). Accordingly, traffic vehicles, coal production and chemical industries from which NO_X is released are the indirect emission sources of nitrate (Zhao et al., 2011; Mooibroek et al., 2011). Higher temperatures could reduce the formation of particulate ammonium nitrate and cause thermal dissociation, as well as volatilization of ammonium nitrate from the particle phase (Li et al., 2014; Russell et al., 1983; Zhao and Gao, 2008; Sun et al., 2015). The nitrate concentration at 220 m was higher than that at 10 m at almost all sizes, which is mainly ascribed to the transport, lower temperature and higher RH at 220 m (Fig. 3).

3.2.4. OC and EC size distributions

As shown in Fig. 5, the size distribution of OC was found to be a bimodal mode that peaked at 1.1–2.1 μm and 3.3–4.7 μm at 10 m, while it was a unimodal pattern with a peaked that shifted slightly to smaller particles (0.7–1.1 μm) at 220 m. The fine-mode OC at 10 m and 220 m accounted for the same proportion (55%) of the OC mass in PM_{10}. EC had a trimodal distribution that peaked at 0.7–1.1 μm, 3.3–4.7 μm and 9–10 μm at both heights. The proportion of fine-mode EC (48%) to the EC mass in PM_{10} at 10 m was higher than that at 220 m (41%).

Combustion sources, biomass burning and exhaust emissions from motor vehicles contribute mostly to the OC in fine particles (Cheng et al., 2013). Coarse-mode OC is mainly attributed to the hygroscopic growth of water-soluble OC (WSOC)-containing particles during transport or the emission of particulate organic carbon (POC) by industrial sources in the surrounding area (Wang et al., 2014a). The EC in fine particles is mainly derived from coal combustion, exhaust emissions and biomass burning from motor vehicles (Zhang et al., 2015). Coarse-mode EC can be formed through the mix of particulate matter and hygroscopic growth during transport, the re-suspension of soil dust and the mechanical friction of vehicle tires (Wang et al., 2014a; Shah et al., 2004; Lan et al., 2011).

The correlation between OC and EC can be used to estimate the anthropogenic origins of carbonaceous aerosols. As shown in Table S2, there was a stronger correlation between OC and EC in fine particles at 10 m and 220 m (R^2 = 0.76 vs. 0.84) compared to that in coarse particles (R^2 = 0.66 vs 0.44). This result indicated that the sources of OC and EC in fine particles were similar, e.g., coal combustion, biomass burning and exhaust emissions (Wang et al., 2014a). However, the weaker correlation between OC and EC in coarse particles meant that the sources of OC and EC in coarse particles were different. Therefore, transport was not the common source of OC and EC in coarse particles.

As shown in Table S3, a good correlation could be found between OC measured at 10 m and 220 m in both fine particles and coarse particles (R^2 = 0.82 vs 0.71), indicating that there were common sources for OC at both heights. A strong correlation of Fine-mode EC measured at 10 m and 220 m could be found (R^2 = 0.62), though the concentration of fine-mode EC at 10 m was 50% higher than that at 220 m. There was a weak correlation between the coarse-mode EC measured at 10 m and 220 m (R^2 = 0.32). This finding suggested that the re-suspension of soil dust and the mechanical friction of vehicle tires contributed the most to the coarse-mode EC at 10 m, while transport could be the major source for the coarse-mode EC at 220 m. In addition, industrial sources could be inferred as the major source of the coarse-mode OC at both heights, when transport has been excluded.

3.3. Source apportionment using PMF

To resolve the appropriate number of factors, different numbers of identifiable sources were tested (Lyu et al., 2016). In this study, four, five, six, and even seven different sources were set in the PMF

Please cite this article in press as: Wang, J., et al., Characterization and source apportionment of size-segregated atmospheric particulate matter collected at ground level and from the urban canopy in Tianjin, Environmental Pollution (2016), http://dx.doi.org/10.1016/j.envpol.2016.10.069

analysis respectively. For six and seven factors, the Q-value (goodness of fit parameter) for this model was not close to the theoretical Q-value. And there were always one or two sources couldn't be given an appropriate physical interpretation. For four and five factors, The Q-value (goodness of fit parameter) was close to the theoretical Q-value. However, larger residuals were found for nitrate when four factors were set. The source profiles were more reasonable when five factors were chosen. Additionally, the measured mass concentrations and the calculated mass concentrations of aerosol particulates showed a high correlation ($R^2 = 0.88$) under five factors. So the best data interpretation was finally achieved with five factors. The obtained source profiles (bars) and contributions (points) of the five factors were presented in Fig. 6.

Section 3.2.4 has shown that carbon could not be ignored in both fine-mode and coarse-mode. As shown in Fig. 7, factor 1 also contributed to the coarse-mode carbon besides fine-mode carbon, especially at 220 m. Combined with Fig. 6, factor 1 primarily consisted of EC, OC, NO_3^- and NO_2^- in fine mode, and some carbon in coarse mode. Sections 3.2.3 and 3.2.4 have mentioned that NO_3^-, NO_2^- and carbon in fine mode is typical for traffic, especially exhaust. Road dust re-suspension, the mix of particulate matter and hygroscopic growth during transport, contribute to the formation of coarse-mode carbon. Therefore the factor was identified as traffic emissions and regional transport.

Factor 2 had a high loading of F^-, Cl^-, NO_3^-, SO_4^{2-}, fine-mode carbon and some coarse-mode OC. (Fig. 6 and Fig. 7). As shown in section 3.2.1, Cl^- was concentrated mostly in fine particles, which

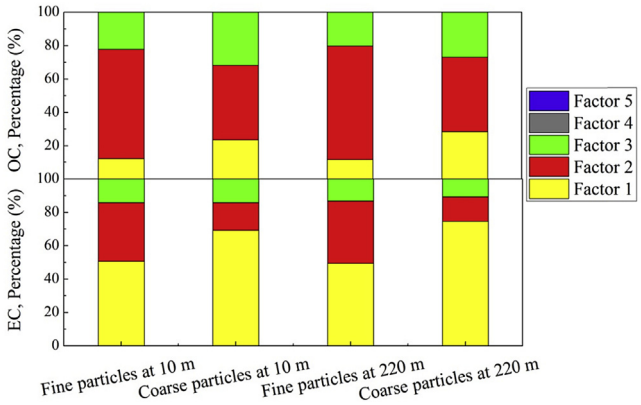

Fig. 7. Contributions of factors to carbonaceous species in PM.

emphasizes the contribution of coal burning and incineration. In addition, the average OC/EC values during this sampling period was 11.2 and 9.0 at 10 m in fine and coarse particles, respectively, which was close to the specific value of coal combustion (12.0) (Cao et al., 2005; Watson et al., 2001). Coal combustion was an important source of atmospheric particles in north of China (Liu et al., 2016), which was generally used for coal-combustion power-plants, industrial enterprises and the domestic heating during winter (Gao et al., 2016; Liu et al., 2016). Thus, it was probably representative of industrial pollution and coal combustion.

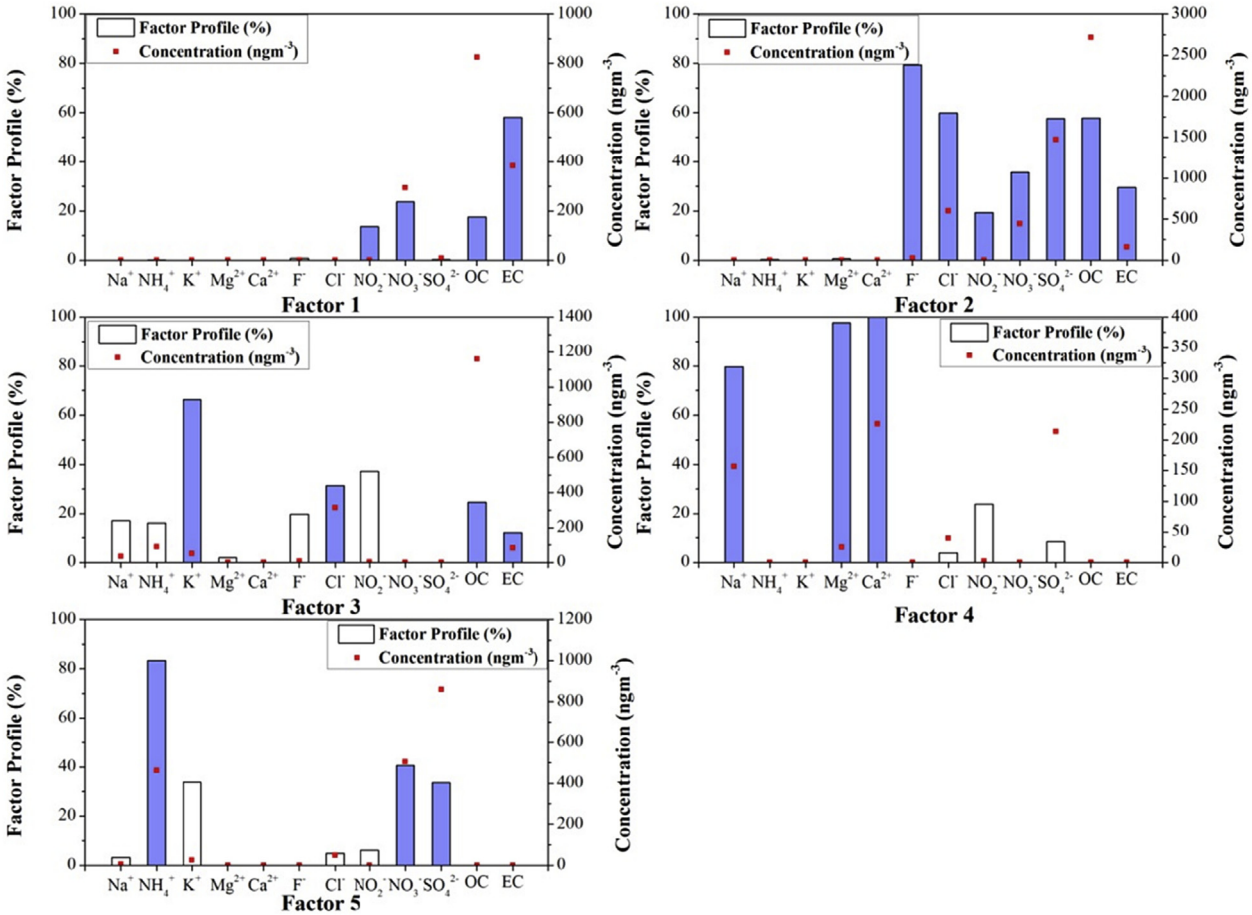

Fig. 6. Source profiles obtained with the PMF for atmospheric particulates. Filled bars identify the species that mainly characterize each factor profile.

Please cite this article in press as: Wang, J., et al., Characterization and source apportionment of size-segregated atmospheric particulate matter collected at ground level and from the urban canopy in Tianjin, Environmental Pollution (2016), http://dx.doi.org/10.1016/j.envpol.2016.10.069

K^+ was a major product of sintering plant stacks (Almeida et al., 2015). Combined with 3.2.1 and 3.2.4, biomass burning contributed to Cl^-, OC and EC besides K^+. Factor 3 was primarily characterized by K^+, OC, EC and Cl^-, and may represent the biomass burning (Lestari and Mauliadi, 2009; Cao et al., 2015; Cheng et al., 2013; Zhang et al., 2015). As mentioned above, the average OC/EC values during the sampling period were larger than 9.0 in particles, Watson et al. (2001) and Cachier et al. (1989) reported that the OC/EC ratios for biomass burning were up to 4.1–14.5. Therefore, biomass burning could make some effects on the particles during winter in Tianjin.

Na^+, Cl^-, Mg^{2+} and Ca^{2+} were relatively high in factor 4. Therefore, it was reasonable to identify this factor as the mix of re-suspended dust and marine salt. Moreover, this factor contributed mostly to the coarse particle at both heights (Fig. 8). More and more buildings were under construction with the rapid development of Tianjin, which lead to the enhanced influence on particles. Tianjin city was near Bohai Bay, so the ambient $PM_{2.5}$ could be affected by the marine salt.

Factor 5 was primarily defined by NH_4^+, NO_3^- and SO_4^{2-}, which could be interpreted as secondary inorganic aerosols (Liu et al., 2016). Secondary inorganic aerosols, which dominate aerosol particles (Fig. 4), are significantly affected by regional transport, especially in the urban canopy (Sun et al., 2014; Zheng et al., 2015; Li et al., 2015). Previous studies have shown that secondary sources played a dominant role for the ambient $PM_{2.5}$ and PM_{10} in Tianjin (Tian et al., 2013).

The relative source contributions to fine particles and coarse particles at 10 m and 220 m are shown in Fig. 8. The contributions of traffic emission and transport (13.1% at 10 m vs. 10.8% at 220 m), re-suspended dust and marine salt (12.6% vs. 11.3%) and biomass burning (4.2% vs. 2.9%) to fine particles apportioned by PMF decreased with the increase in vertical height, while the reverse was true for industrial pollution and coal combustion (44.6% vs. 44.8%) and secondary inorganic aerosols (25.5% vs. 30.2%). The contributions of industrial pollution and coal combustion (31.5% vs. 31.2%) and biomass burning (2.1% vs. 2.0%) for coarse particles were similar. The contributions of secondary inorganic aerosols (6.8% vs. 11.1%) and traffic emissions and transport (12.0% at 10 m vs. at 220 m 14.5%) for coarse particles increased with the increase in vertical height, while the reverse was true for re-suspended dust and marine salt (47.6% vs.41.2%).

The contribution of factor 1 (traffic emission and transport) to fine particles at 10 m was higher than that at 220 m, while the regularity was reverse for coarse particles. Sections 3.2.3 and 3.2.4 have mentioned that traffic emission contributed mostly to fine mode chemical compositions and was the typical local source of PM. Accordingly, transport played an important role on the higher contribution of factor 1 to coarse particles at the urban canopy compared to that at ground level. The comprehensive influence of the chimney stacks of factories and burning crude coal by residents resulted in the similar contributions of factor 2 (industrial pollution and coal combustion) to PM at the two different heights. Factor 3 (biomass burning) contributed least to PM at both heights compared with other sources. However, it could have an effect on fine particles at ground level. The larger size of Factor 4 (re-suspended dust and marine salt) may contribute to the decrease with the increase in vertical height. The contribution of Factor 5 (secondary inorganic aerosols) to PM at 220 m was higher than that at 10 m, indicating that it was affected by regional transport. The average trajectories of four clusters were shown in Fig. 9. All trajectories originated from the northwest of Tianjin. Cluster 2 was composed the most frequent trajectories (accounting for 38% of the observations) and originated from Hebei Province. Cluster 1 and cluster 3, accounting for 40% of the observations, included trajectories from Mongolia and Hebei Province. Cluster 4 (23%) spent much of the time over the Mongolia, Hebei Province and Beijing. It was suggested that Factor 1 and Factor 5 at the urban canopy in Tianjin was affected by regional transport from Hebei Province and Beijing. As with the previous study (Han et al., 2015), with the increase of vertical height, the influence of traffic emissions, re-suspended dust and biomass burning on PM weakens, but the characteristics of regional transport gradually become obvious.

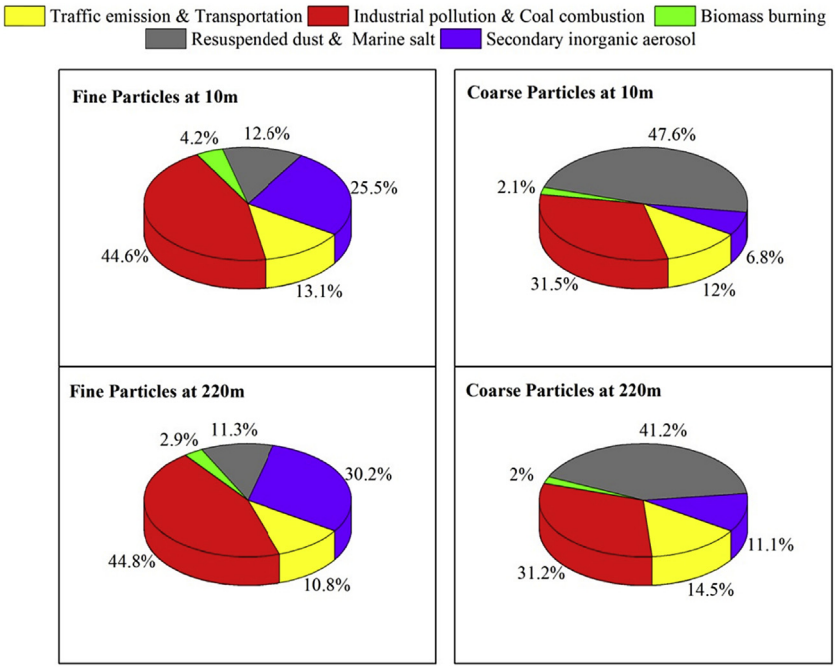

Fig. 8. Source apportionment of fine particles and coarse particles at 10 m and 220 m.

Please cite this article in press as: Wang, J., et al., Characterization and source apportionment of size-segregated atmospheric particulate matter collected at ground level and from the urban canopy in Tianjin, Environmental Pollution (2016), http://dx.doi.org/10.1016/j.envpol.2016.10.069

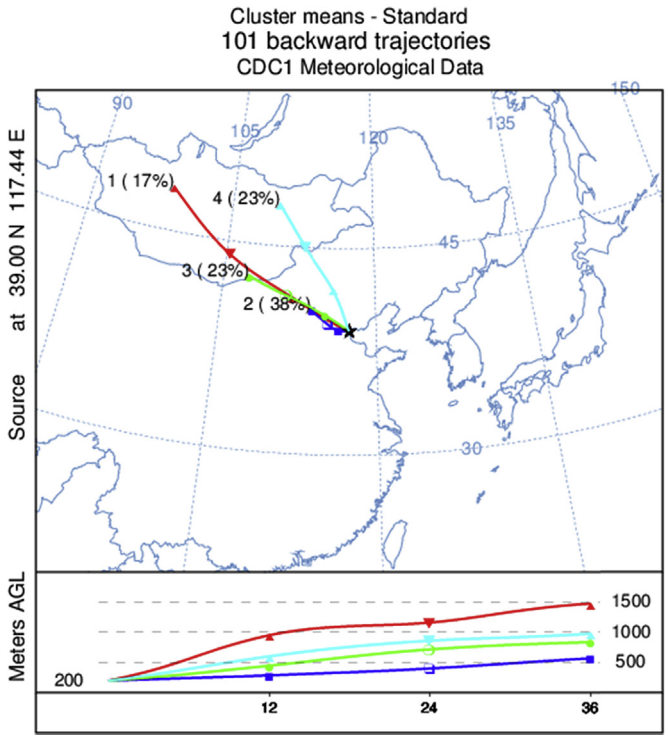

Fig. 9. Air mass backward trajectories at receptor heights of 200 m above the ground level at the sampling site.

4. Conclusions

The concentrations and size distributions of chemical compositions and sources of PM at the urban canopy were affected by regional transport due to a stable layer at approximately 200 m and higher WS at 220 m. A similar bimodal distribution of PM mass concentrations could be found at two different heights, which peaked at 0.7–1.1 μm and 9.0–10.0 μm, respectively. OC, SO_4^{2-}, NO_3^-, Cl^-, NH_4^+ and EC were the principal chemical compositions of PM at the two different heights. The proportion of ions and carbonaceous species in PM rose with the increase in height, in particular for SO_4^{2-} and NO_3^-. The concentrations of PM, Cl^- and EC in fine particles at 10 m were higher than that at 220 m, while the reverse was true for NO_3^- and SO_4^{2-}. The concentrations of Na^+, Ca^{2+}, Mg^{2+}, Cl^- and EC in coarse particles at 10 m were higher than that at 220 m.

The size distributions of major primary species, such as Cl^-, Na^+, Ca^{2+}, Mg^{2+} and EC, were similar at the two different heights, indicating that they were common and dominant sources at ground level and in the urban canopy. Na^+ was mainly derived from sea salt. Cl^- was mainly derived from coal burning, biomass burning and a portion of sea salt. Ca^{2+} and Mg^{2+} mainly came from soil particles or falling dust. The size distributions of SO_4^{2-}, NH_4^+, NO_3^- and OC, which were partly secondary generated species, were different at both heights, indicating that there were different formation mechanisms. The secondary sources and coal burning contributed mostly to the sulfate at 10 m, in which long-range transport was another source for secondary sulfate at 220 m. Nitrate was mainly derived from vehicles and secondary sources at 10 m, while long-range transport was another source for secondary nitrate at 220 m. OC and EC in fine particles were mainly derived from combustion sources and vehicles at both heights. Resuspension of soil dust and mechanical friction of vehicle tires contributed mostly to the Coarse-mode EC at 10 m, while transport was the major source for the Coarse-mode EC at 220 m. Industrial emissions were inferred as the major source of Coarse-mode OC at both heights.

Industrial pollution and coal combustion (44.6% vs. 44.8%), secondary inorganic aerosols (25.5% vs. 30.2%), traffic emissions and transport (13.1% at 10 m vs. 10.8% at 220 m) and re-suspended dust and marine salt (12.6% vs. 11.3%) were the major sources of fine particles at 10 m and 220 m. Re-suspended dust and marine salt (47.6% vs.41.2%), industrial pollution and coal combustion (31.5% vs. 31.2%), traffic emissions and transport (12.0% at 10 m vs. at 220 m 14.5%) and secondary inorganic aerosols (6.8% vs. 11.1%) were the major sources for coarse particles at 10 m and 220 m. With the increase in vertical height, the influence of traffic emissions, re-suspended dust and biomass burning on PM weakened, but the characteristics of regional transport from Hebei Province and Beijing gradually become obvious. However, the 220 m height was influenced by local emissions, which may be not high enough to reflect the background levels of pollutants in the atmospheric boundary layer.

Acknowledgements

We would like to thank Tianjin Meteorological Bureau for the supporting. The collection and analysis of data used in this work was also supported by the National Natural Science Foundation of China [grant number 41205089]; Tianjin Science and Technology Project [grant numbers 14ZCDGSF00027, 14ZCDGSF00029].

Appendix A. Supplementary data

Supplementary data related to this article can be found at http://dx.doi.org/10.1016/j.envpol.2016.10.069

References

Almeida, S.M., Lage, J., Fernández, B., Garcia, S., Reis, M.A., Chaves, P.C., 2015. Chemical characterization of atmospheric particles and source apportionment in the vicinity of a steelmaking industry. Sci. Total Environ. 521, 411–420.
Amato, F., Pandolfi, M., Escrig, A., Querol, X., Alastuey, A., Pey, J., 2009. Quantifying road dust resuspension in urban environment by multilinear engine: a comparison with PMF2. Atmos. Environ. 43, 2770–2780.
Ancelet, T., Davy, P.K., Mitchell, T., Trompette, W.J., Markwitz, A., Weatherburn, D.C., 2012. Identification of particulate matter sources on an Hourly time-scale in a wood burning community. Environ. Sci. Technol. 46, 4767–4774.
Anlauf, K., Li, S.M., Leaitch, R., Brook, J., Hayden, K., ToomSauntry, D., Wiebe, A., 2006. Ionic composition and size characteristics of particles in the lower Fraser Vellay: Pacific 2001 field study. Atmos. Environ. 40, 2662–2675.
Appel, B.R., Tokiwa, Y., Haik, M., Kothny, E.L., 1984. Artifact of particulate sulfate and nitrate formation on filter media. Atmos. Environ. 18, 409–416.
Arimoto, R., Duce, R.A., Savoie, D.L., Prospero, J.M., Talbot, R., Cullen, J.D., Tomza, U., Lewis, N.F., Ray, B.J., 1996. Relationships among aerosol compositions from Asia and the North Pacific during Pem-West. J. Geophys. Res. 101 (D1), 2011–2023.
Bellouin, N., Boucher, O., Haywood, J., Reddy, M.S., 2005. Global estimate of aerosol direct radiative forcing from satellite measurements. Nature 438, 1138–1141.
Cachier, H., Bremond, M.P., Buatmenard, P., 1989. Carbonaceous aerosols from different tropical biomass burning sources. Nature 340, 371–373.
Cao, J.J., Wu, F., Chow, J.C., Lee, S.C., Li, Y., Chen, S.W., An, Z.S., Fung, K.K., Watson, J.G., Zhu, C.S., Liu, S.X., 2005. Characterization and source apportionment of atmospheric organic and elemental carbon during fall and winter of 2003 in Xi'an, China. Atmos. Chem. Phys. 5, 3127–3137.
Cao, F., Zhang, S.C., Kawamura, K., Zhang, Y.L., 2015. Inorganic markers, carbonaceous components and stable carbon isotope from biomass burning aerosols in Northeast China. Sci. Total Environ. 24 (3), 671–682.
Chan, Y.C., Vowles, P.D., McTainsh, G.H., Simpson, R.W., Cohen, D.D., Bailey, G.M., McOrist, G.D., 2000. Characterisation and source identification of PM_{10} aerosol samples collected with a high volume cascade impactor in Brisbane (Australia). Sci. Total Environ. 262, 5–19.
Cheng, Y., Engling, G., He, K.B., Duan, F.K., Ma, Y.L., Du, Z.Y., Liu, J.M., Zheng, M., Weber, R.J., 2013. Biomass Burn. contribution Beijing aerosol Atmos. Chem. Phys. 13, 7765–7781.
Chueinta, W., Hopke, P.K., Paatero, P., 2000. Investigation of sources of atmospheric aerosol at urban and suburban residential areas in Thailand by positive matrix factorization. Atmos. Environ. 34, 3319–3329.
Contini, D., Cesari, D., Genga, A., Siciliano, M., Ielpo, P., Guascito, M.R., Conte, M., 2014. Source apportionment of size-segregated atmospheric particles based on

the major water-soluble components in Lecce (Italy). Sci. Total Environ. 472, 248–261.
Dasch, J.M., Cadle, S.H., Kennedy, K.G., Mulawa, P.A., 1989. Comparison of annular denuders and filter packs for atmospheric sampling. Atmos. Environ. 23, 2775–2782.
Deng, X.J., Li, F., Li, Y.H., Li, J.Y., Huang, H.Z., Liu, X.T., 2015. Vertical distribution characteristics of PM in the surface layer of Guangzhou. Particuology 20, 3–9.
Gao, W.K., Tang, G.J., Yao, Q., Liu, Z.R., Wang, H., Wang, Y.S., 2012. Vertical distribution of air pollutants during serious air pollution event in Tianjin. Res. Environ. Sci. 25 (7), 731–738 (in Chinese).
Gao, J., Peng, X., Chen, G., Xu, J., Shi, G.L., Zhang, Y.C., Feng, Y.C., 2016. Insights into the chemical characterization and sources of $PM_{2.5}$ in Beijing at a 1-h time resolution. Sci. Total Environ. 542, 162–171.
Gietl, J.K., Klemm, O., 2009. Source identification of size-segregated aerosol in münster, Germany, by factor analysis. Aerosol Sci. Technol. 43 (8), 828–837.
Han, S.Q., Zhang, Y.F., Wu, J.H., Zhang, X.Y., Tian, Y.Z., Wang, Y.M., Ding, J., Yan, W.Q., Bi, X.H., Shi, G.L., Yao, Q., Huang, H.Y., Feng, Y.C., 2015. Evaluation of regional background particulate matter concentration based on vertical distribution characteristics. Atmos. Chem. Phys. 15, 11165–11177.
Harrison, R.M., Sturges, W.T., Kitto, A.M.N., Li, Y., 1990. Kinetics of evaporation of ammonium chloride and ammonium nitrate aerosols. Atmos. Environ. 24 A, 1883–1888.
Heeinrich, J., Pitz, M., Bischof, W., Krug, N., Borm, P.J.A., 2003. Endotoxin in fine ($PM_{2.5}$) and coarse ($PM_{2.5\text{-}10}$) particle mass of ambient aerosols. A temporo-spatial analysis. Atmos. Environ. 37, 3659–3667.
Hering, S.V., Friedlander, S.K., 1982. Origins of aerosol sulfur size distributions in the Los Angeles Basin. Atmos. Environ. 16, 2647–2656.
Hering, S., Eldering, A., Seinfeld, J.H., 1997. Bimodal character of accumulation mode aerosol mass distributions in Southern California. Atmos. Environ. 31, 1–11.
Herner, J.D., Ying, Q., Aw, J., Gao, O., Chang, D.P.Y., Kleeman, M., 2006. Dominant mechanisms that shape the airborne particle size and composition in central California. Aerosol Sci. Technol. 40, 827–844.
Huang, H., Sun, M.L., Liu, A.X., Zhang, C.C., 2009. Vertical distribution of air pollutants in the atmosphere in Tianjin. Acta Sci. Circumstantiae 29 (12), 2478–2483 (in Chinese).
Huang, R.J., Zhang, Y.L., Bozzetti, C., Ho, K.F., Cao, J.J., Han, Y.M., Daellenbach, K.R., Slowik, J.G., Platt, S.M., Canonaco, F., Zotter, P., Wolf, R., Pieber, S.M., Bruns, E.A., Crippa, M., Ciarelli, G., Piazzalunga, A., Schwikowski, M., Abbaszade, G., Schnelle-Kreis, J., Zimmermann, R., An, Z.S., Szidat, S., Baltensperger, U., El Haddad, I., Prevot, A.S.H., 2014. High secondary aerosol contribution to particulate pollution during haze events in China. Nature 514, 218–222.
Ian Colbeck, Z.A.N., 2010. Assessment of bacterial and fungal aerosol in different residential settings. Water, Air, Soil Pollut. 211, 367–377.
Ian Colbeck, Z.A.N., 2012. Winter time concentrations and size distribution of bio-aerosols in different residential settings in the UK. Water, Air, Soil Pollut. 223, 5613–5622.
John, W., Wall, S.M., Ondo, J.L., Winklmayr, W., 1990. Modes in the size distributions of atmospheric inorganic aerosol. Atmos. Environ. 24A, 2349–2359.
Kaneyasu, N., Yoshikado, H., Sakamoto, K., Soufuku, M., 1999. Chemical forms and sources of extremely high nitrate and chloride in winter aerosol pollution in Kanto Plain of Japan. Atmos. Environ. 33, 1745–1756.
Kleeman, M.J., Schauer, J.J., Cass, G.R., 1999. Size and composition distribution of fine particulate matter emitted from wood burning, meat charbroiling and cigarettes. Environ. Sci. Technol. 33, 3516–3523.
Kumar, A., Sarin, M.M., Sudheer, A.K., 2008. Mineral and anthropogenic aerosols in Arabian Sea-atmospheric boundary layer: sources and spatial variability. Atmos. Environ. 42, 5169–5181.
Lan, Z.J., Chen, D.L., Li, X., Huang, X.F., He, L.Y., Denga, Y.G., Feng, N., Hu, M., 2011. Modal characteristics of carbonaceous aerosol size distribution in an urban atmosphere of South China. Atmos. Res. 100, 51–60.
Lestari, P., Mauliadi, Y.D., 2009. Source apportionment of particulate matter at urban mixed site in Indonesia using PMF. Atmos. Environ. 43, 1760–1770.
Li, Y., Schwandner, F.M., Sewell, H.J., Zivkovich, A., Tigges, M., Raja, S., Holcomb, S., Molenar, J.V., Sherman, L., Archuleta, C., Lee, T., Collett, J.L., 2014. Observations of ammonia, nitric acid, and fine particles in a rural gas production region. Atmos. Environ. 83, 80–89.
Li, P., Yan, R., Yu, S., Wang, S., Liu, W., Bao, H., 2015. Reinstate regional transport of $PM_{2.5}$ as a major cause of severe haze in Beijing. Proc. Natl. Acad. Sci. 112 (21), 2739–2740.
Liu, B.S., Song, N., Dai, Q.L., Mei, R.B., Sui, B.H., Bi, X.H., Feng, Y.C., 2016. Chemical composition and source apportionment of ambient $PM_{2.5}$ during the non-heating period in Taian, China. Atmos. Res. 170, 23–33.
Long, S.L., Zeng, J.R., Li, Y., Bao, L.M., Cao, L.L., Liu, K., Xu, L., Lin, J., Liu, W., Wang, G.H., Yao, J., Ma, C.Y., Zhao, Y.D., 2014. Characteristics of secondary inorganic aerosol and sulfate species in size-fractionated aerosol particles in Shanghai. J. Environ. Sci. 26, 1040–1051.
Lyu, X.P., Chen, N., Guo, H., Zeng, L.W., Zhang, W.H., Shen, F., Quan, J.H., Wang, N., 2016. Chemical characteristics and causes of airborne particulate pollution in warm seasons in Wuhan, central China. Atmos. Chem. Phys. 16 (16), 1–35.
Mooibroek, D., Schaap, M., Weijers, E.P., Hoogerbrugge, R., 2011. Source apportionment and spatial variability of $PM_{2.5}$ using measurements at five sites in The Netherlands. Atmos. Environ. 45, 4180–4191.
Ondov, J.M., Wexler, A.S., 1998. Where do particulate toxins reside? An improved paradigm for the structure and dynamics of the urban mid-Atlantic aerosol. Environ. Sci. Technol. 32, 2547–2555.
Paatero, P., Hopke, P.K., 2003. Discarding or downweighting high-noise variables in factor analytic models. Anal. Chim. Acta 490, 277–289.
Paatero, P., Tapper, U., 1993. Analysis of different modes of factor analysis as least squares fit problems. Chemom. Intelligent Laboratory Syst. 18, 183–194.
Paatero, P., Tapper, U., 1994. Positive matrix factorization: a non-negative factor model with optimal utilization of error estimates of data values. Environmetrics 5, 111–126.
Pathak, R.K., Chan, C.K., 2005. Inter-particle and gas-particle interactions in sampling artifacts of $PM_{2.5}$ in filter-based samplers. Atmos. Environ. 39, 1597–1607.
Pope, C.A., Dockery, D.W., 2006. Health effects of fine particulate air pollution: lines that connect. J. Air Waste Manag. Assoc. 56, 709–742.
Quinn, P.K., Coffman, D.J., Bates, T.S., Welton, E.J., Covert, D.S., Miller, T.L., Johnson, J.E., Maria, S., Russell, L., Arimoto, R., Carrico, C.M., Rood, M.J., Anderson, J., 2004. Aerosol optical properties measured on board the Ronald H. Brown during ACE-Asia as a function of aerosol chemical composition and source region. J. Geophys. Res. 109, D19S01.
Ramachandran, S., Kedia, S., 2010. Black carbon aerosols over an urban region: radiative forcing and climate impact. J. Geophys. Res. - Atmos. 115, D10202.
Russell, A.G., McRae, G.J., Cass, G.R., 1983. Mathematical modeling of the formation and transport of ammonium nitrate aerosol. Atmos. Environ. 17, 949–964.
Sannigrahi, P., Sullivan, A., Weber, R., Ingall, E., 2006. Characterization of water-soluble organic carbon in urban atmospheric aerosols using solid-state ^{13}C NMR spectroscopy. Environ. Sci. Technol. 40, 666–672.
Shah, S.D., Cocker, D.R., Miller, J.W., Norbeck, J.M., 2004. Emission rates of particulate matter and elemental and organic carbon from In-use diesel engines. Environ. Sci. Technol. 38 (9), 2544–2550.
Shen, Z.X., Arimoto, R., Cao, J.J., Zhang, R.J., Li, X.X., Du, N., Okuda, T., Nakao, S., Tanaka, S., 2008. Seasonal variations and evidence for the effectiveness of pollution controls on water-soluble inorganic species in total suspended particulates and fine particulate matter from Xi'An, China. J. Air & Waste Manag. Assoc. 58, 1560–1570.
Shi, G.L., Tian, Y.Z., Han, S.Q., Zhang, Y.F., Li, X., Feng, Y.C., Wu, J.H., Zhu, T., 2012. Vertical characteristics of carbonaceous species and their source contributions in a Chinese mega city. Atmos. Environ. 60, 358–365.
Song, X.H., Polissar, A.V., Hopke, P.K., 2001. Sources of fine particle composition in the northeastern US. Atmos. Environ. 35 (31), 5277–5286.
Sun, Y.L., Jiang, Q., Wang, Z.F., Fu, P.Q., Li, J., Yang, T., Yin, Y., 2014. Investigation of the sources and evolution processes of severe haze pollution in Beijing in January 2013. J. Geophys. Res. 119, 4380–4398.
Sun, Y.L., Du, W., Wang, Q.Q., Zhang, Q., Chen, C., Chen, Y., Chen, Z.Y., Fu, P.Q., Wang, Z.F., Gao, Z.Q., Worsnop, D.R., 2015. Real-time characterization of aerosol particle composition above the urban canopy in Beijing: insights into the interactions between the atmospheric boundary layer and aerosol chemistry. Environ. Sci. Technol. 49 (19), 11340–11347.
Sun, Y.L., Chen, C., Zhang, Y.J., Xu, W.Q., Zhou, L.B., Cheng, X.L., Zheng, H.T., Ji, D.S., Li, J., Tang, X., Fu, P.Q., Wang, Z.F., 2016. Rapid formation and evolution of an extreme haze episode in Northern China during winter 2015. Sci. Rep. 6, 27151.
Tan, J.H., Duan, J.C., Chai, F.H., He, K.B., Hao, J.M., 2014. Source apportionment of size segregated fine/ultrafine particle by PMF in Beijing. Atmos. Res. 139, 90–100.
Tian, Y.Z., Shi, G.L., Han, S.Q., Zhang, Y.F., Feng, Y.C., Liu, G.R., Gao, L.J., Wu, J.H., Zhu, T., 2013. Vertical characteristics of levels and potential sources of water-soluble ions in PM_{10} in a Chinese megacity. Sci. Total Environ. 447, 1–9.
Viana, M., Pandolfi, M., Minguillón, M.C., Querol, X., Alastuey, A., Monfort, E., Celades, I., 2008. Inter-comparison of receptor models for PM source apportionment: case study in an industrial area. Atmos. Environ. 42, 3820–3832.
Wang, T., Xie, S.D., 2009. Assessment of traffic-related air pollution in the urban streets before and during the 2008 Beijing Olympic Games traffic control period. Atmos. Environ. 43, 5682–5690.
Wang, Y., Zhuang, G.S., Tang, A., Yuan, H., Sun, Y.L., Chen, S., Zheng, A.H., 2005. The ion chemistry and source of $PM_{2.5}$ aerosol in Beijing. Atmos. Environ. 39, 3771–3784.
Wang, H.L., Zhu, B., An, J.L., Duan, Q., Zou, J.N., Shen, L.J., 2014a. Size distribution and characterization of OC and EC in atmospheric aerosols during the Asian youth games of Nanjing, China. J. Environ. Sci. 35, 3271–3279 (in Chinese).
Wang, L.T., Wei, Z., Yang, J., Zhang, Y., Zhang, F.F., Su, J., Meng, C.C., Zhang, Q., 2014b. The 2013 severe haze over the southern Hebei, China: model evaluation, source apportionment, and policy implications. Atmos. Chem. Phys. 14, 3151–3173.
Wang, Y., Yao, L., Wang, L., Liu, Z., Ji, D., Tang, G., Zhang, J., Sun, Y., Hu, B., Xin, J., 2014c. Mechanism for the formation of the January 2013 heavy haze pollution episode over central and eastern China. Sci. China Earth Sci. 57 (1), 14–25 (in Chinese).
Watson, J.G., 2002. Visibility: science and regulation. J. Air Waste Manag. Assoc. 52, 628–713.
Watson, J.G., Chow, J.C., Houck, J.E., 2001. $PM_{2.5}$ chemical source profiles for vehicle exhaust, vegetative burning, geological material, and coal burning in Northwestern Colorado during 1995. Chemosphere 43, 1141–1151.
Whitby, K.T., 1978. The physical characteristics of sulfur aerosols. Atmos. Environ. 12, 135–159.
Wu, H., Zhang, Y.F., Han, S.Q., Wu, J.H., Bi, X.H., Shi, G.L., Wang, J., Yao, Q., Cai, Z.Y., Liu, J.L., Feng, Y.C., 2015. Vertical characteristics of $PM_{2.5}$ during the heating season in Tianjin, China. Sci. Total Environ. 523, 152–160.
Xue, M., Ma, J.Z., Yan, P., Pan, X.L., 2011. Impacts of pollution and dust aerosols on the atmospheric optical properties over a polluted rural area near Beijing city. Atmos. Res. 101, 835–843.
Yamasoe, M.A., Artaxo, P., Miguel, A.H., Allen, A.G., 2000. Chemical composition of

Please cite this article in press as: Wang, J., et al., Characterization and source apportionment of size-segregated atmospheric particulate matter collected at ground level and from the urban canopy in Tianjin, Environmental Pollution (2016), http://dx.doi.org/10.1016/j.envpol.2016.10.069

aerosol particles from direct emissions of vegetation fires in the Amazon Basin: watersoluble species and trace elements. Atmos. Environ. 34, 1641–1653.
Yang, Y.J., Zhou, R., Wu, J.J., Yu, Y., Ma, Z.Q., Zhang, L.J., Di, Y.A., 2015. Seasonal variations and size distributions of water-soluble ions in atmospheric aerosols in Beijing, 2012. J. Environ. Sci. 34, 197–205.
Yang, H., Chen, J., Wen, J., Tian, H., Liu, X., 2016. Composition and sources of $PM_{2.5}$ around the heating periods of 2013 and 2014 in Beijing: implications for efficient mitigation measures. Atmos. Environ. 124, 1–9.
Yao, X.H., Lau, A.P.S., Fang, M., Chan, C.K., Hu, M., 2003. Size distributions and formation of ionic species in atmospheric particulate pollutants in Beijing, China: 1-inorganic ions. Atmos. Environ. 37, 2991–3000.
Zhang, Y.L., Schnelle-Kreis, J., Abbaszade, G., Zimmermann, R., Zotter, P., Shen, R.R., Schäfer, K., Shao, L., Prévôt, A.S.H., Szidat, S., 2015. Source apportionment of elemental carbon in Beijing, China: insights from radiocarbon and organic marker measurements. Environ. Sci. Technol. 49, 8408–8415.
Zhao, Y.L., Gao, Y., 2008. Mass size distributions of water-soluble inorganic and organic ions in size-segregated aerosols over metropolitan Newark in the US east coast. Atmos. Environ. 42, 4063–4078.
Zhao, J.P., Zhang, F.W., Chen, J.S., Xu, Y., 2010. Characterization of polycyclic aromatic hydrocarbons and gas/particle partitioning in a coastal city, Xiamen, Southeast China. J. Environ. Sci. 22, 1014–1022.
Zhao, J.P., Zhang, F.W., Xu, Y., Chen, J.S., 2011. Characterization of water-soluble inorganic ions in size-segregated aerosols in coastal city. Xiamen. Atmos. Res. 99, 546–562.
Zheng, G.J., Duan, F.K., Su, H., Ma, Y.L., Cheng, Y., Zheng, B., Zhang, Q., Huang, T., Kimoto, T., Chang, D., Pöschl, U., Cheng, Y.F., He, K.B., 2015. Exploring the severe winter haze in Beijing: the impact of synoptic weather, regional transport and heterogeneous reactions. Atmos. Chem. Phys. 15, 2969–2983.
Zhuang, H., Chan, C.K., Fang, M., Wexler, A.S., 1999. Size distributions of particulate sulfate, nitrate, and ammonium at a coastal site in Hong Kong. Atmos. Environ. 33, 843–853.
Zíkova, N., Wang, Y.G., Yang, F.M., Li, X.H., Tian, M., Hopke, P.K., 2015. On the source contribution to Beijing $PM_{2.5}$ concentrations. Atmos. Environ. 134, 84–95.

Please cite this article in press as: Wang, J., et al., Characterization and source apportionment of size-segregated atmospheric particulate matter collected at ground level and from the urban canopy in Tianjin, Environmental Pollution (2016), http://dx.doi.org/10.1016/j.envpol.2016.10.069